iJRASET
International Journal For Research in Applied Science and Engineering Technology

INTERNATIONAL JOURNAL FOR RESEARCH

IN APPLIED SCIENCE & ENGINEERING TECHNOLOGY

Volume: 5 **Issue:** XI **Month of publication:** November 2017

DOI:

www.ijraset.com

Call: 08813907089 | E-mail ID: ijraset@gmail.com

International Journal for Research in Applied Science & Engineering Technology (IJRASET)
ISSN: 2321-9653; IC Value: 45.98; SJ Impact Factor:6.887
Volume 5 Issue XI November 2017- Available at www.ijraset.com

Free Vibration Behavior of FG-CNT Reinforced Composite Plates Using Higher Order Shear Deformation Theory

Lakshmi Chaitanya Kolli[1], J. Suresh Kumar[1]
[1]*Department of Mechanical Engineering, JNTUH College of Engineering, J.N.T.University, Hyderabad*

Abstract: ***This research aims at studying the free vibration analysis of CNT reinforced functionally graded composite rectangular plate using higher order shear deformation theory. The equations of motion of the structural system are derived using the Hamilton's principle. The vibration characteristics of the model in the closed form are obtained by using Navier's method under simply supported boundary conditions. The fundamental frequency of FG-CNT reinforced composite rectangular plate under the given boundary conditions is presented for different aspect ratios. The present results are compared with the solutions of the other HSDTs available in the literature. It can be concluded that the proposed theory is accurate and efficient in predicting the vibration behaviour of FG-CNT plates.***
Keywords: Vibration Behavior, FG-CNT Plates, Effective Material Properties, HSDT, Navier's Method.

I. INTRODUCTION

Functionally graded materials (FGMs) are multifunctional composites involving spatially varying volume fraction of constituent materials, thus providing a graded microstructure and macro-properties. CNT is an effective reinforcement material in the case of composite material developments, owing to its good physical and chemical properties. Guided by the concept of functionally graded (FG) materials, a class of new emerging composite materials, the FG-CNT reinforced composite, has been proposed making use of CNTs as the reinforcements in a functionally graded pattern. Using a powder metallurgy fabrication process, carbon-nanotube-reinforced composites (CNTRCs) may be achieved with a non-uniform distribution of CNTs through the media. This type of reinforced composite media is known as functionally graded carbon-nanotube-reinforced composite (FG-CNTRC). This new type of FG-CNT reinforced composite will need further research so as to find out its mechanical properties.

The advantages of FG-CNT include multi-functionality, ability to withstand at high pressures and in harsh environments, resistant to wear and tear and ability to remove stress concentrations. Using FG-CNT, intricate shapes can be easily produced and it has Cost-effective manufacturing processes. FG-CNTs have wide applications in aerospace structures to withstand aero-thermal loads [4]. They are used as a reactor shield in nuclear reactors to reduce chemical corrosion and thermal stress and also as TBCs in combustion chambers. It is used in manufacturing the components of propulsion system, submarines, and for cutting tools.

II. LITERATURE REVIEW

The buckling, vibration, linear and nonlinear bending behaviours of FG-CNT reinforced composite structures have attracted much attention from researchers [7]. Using HSDT theory, L.W. Zhang et al.[3] studied the vibration analysis of FG-CNT reinforced composite plates subjected to in-plane loads based on State-space Levy method. Mohammad Rahim Nami et al.[7] investigated the free vibration of thick functionally graded carbon nanotube-reinforced rectangular composite plates based on three dimensional elasticity theory via differential quadrature method.Based on the first-order shear deformation plate theory, Zhu et al.[8] carried out bending and free vibration analyses of thin-to-moderately thick FG composite plates reinforced by single-walled carbon nanotubes.Results revealed the influences of the volume fractions of CNT and the edge -to- thickness ratios on the bending responses, natural frequencies and mode shapes of FG-CNTRC plates. A first known free vibration characteristics of functionally graded nano-composite triangular plates reinforced by single-walled carbon nanotubes (SWCNTs) is presented by L.W. Zhang et al.[9]. They studied the free vibration analysis of functionally graded carbon nanotube reinforced composite triangular plates using the FSDT and element-free IMLS-Ritz method.

Liao-Liang Ke et al.[10] investigated the Nonlinear free vibration of functionally graded carbon nanotube-reinforced composite beams. Based on Timoshenko beam theory and von Kármán geometric nonlinearity, the nonlinear free vibration of functionally graded nanocomposite beams reinforced by single-walled carbon nanotubes (SWCNTs) were studied. They also investigate the

©IJRASET (UGC Approved Journal): All Rights are Reserved

effects of nanotube volume fraction, vibration amplitude, slenderness ratio, end supports and CNT distribution on the nonlinear free vibration characteristics of FGCNTRC beams. Yas et al. [11] investigated the three-dimensional vibration properties of FG-CNT reinforced composite cylindrical panels reinforced with single-walled carbon nanotubes. The results showed that the distribution and volume fractions of CNTs have a significant effect on normalized natural frequency. Heshmati et al. [12] studied the effects of carbon nanotube length, waviness, agglomeration and distribution on the vibration behaviour of functionally graded nano composite beams reinforced by carbon nanotubes. T. Kant and K. Swaminathan [13] presented the analytical formulations and solutions to the natural frequency analysis of simply supported composite and sandwich plates using higher order shear deformation theory. The equations are formulated using Hamilton's principle and are solved by the Taylor's series of Navier's solution.

The present paper deals with the analytical formulations and solutions for the vibration analysis of FG-CNT reinforced composite plate using higher order shear deformation theory (HSDT) without enforcing zero transverse shear stress on the top and bottom surfaces of the plate. The theoretical model presented herein incorporates the transverse extensibility which accounts for the transverse effects. Thus a shear correction factor is not required. The plate material is graded through the thickness direction. The plate's governing equations and its boundary conditions are derived by employing the principle of virtual work. Solutions are obtained for FG-CNT reinforced composite plate in closed-form using Navier's technique and solving the Eigen value equation. The present results are compared with the solutions of the other HSDTs available in the literature to verify the accuracy of the proposed theory in predicting the natural frequencies of FG-CNT reinforced composite plate. The effects of side-to-thickness ratios and volume fraction exponent on the natural frequencies are studied after establishing the accuracy of the present results for FG-CNT reinforced composite plate.

III. FORMULATION OF THE EQUATIONS OF MOTION

The FG-CNT reinforced composite plate shown in Fig.2 is studied in this investigation. The plate is subjected to simply supported boundary conditions. The length, width and thickness of the FG-CNT reinforced composite plate are a, band h respectively.Two types of distributions for the CNTs in the FG-CNT reinforced composite plates are studied, and these CNT configurations are displayed in Fig.1, where the uniform distribution and the other CNT distribution are denoted by UD and FGX respectively. In FGX, both the top and bottom surfaces of the plate are CNT-rich.

The volume fractions of the three distribution types are expressed as follows:

$$V_{CNT}(z) = V^*_{CNT}\ , \text{(UD)}$$
$$V_{CNT}(z) = \frac{4|z|}{h} V^*_{CNT}, \text{(FGX)} \qquad \text{..... (1)}$$

where $V^*_{CNT} = \frac{m_{CNT}}{m_{CNT}+(\rho^{CNT}/\rho^m)-(\rho^{CNT}/\rho^m)m_{CNT}}$

in which m_{CNT} is the fraction of mass of the CNTs, and ρ^m and ρ^{CNT} are densities of the matrix and CNTs.

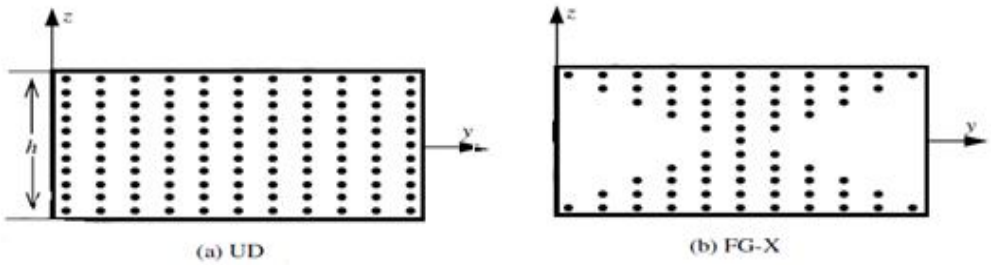

Fig.1 Schematic diagram of the two distributions of CNT.

The effective Young's moduli and Poisson's ratio are calculated by

$$E_{11} = \eta_1 V_{CNT}(z) E_{11}^{CNT} + V_m(z) E^m$$

$$\frac{\eta_2}{E_{22}} = \frac{V_{CNT}(z)}{E_{22}^{CNT}} + \frac{V_m(z)}{E^m}$$

$$\frac{\eta_3}{G_{12}} = \frac{V_{CNT}(z)}{G_{12}^{CNT}} + \frac{V_m(z)}{G^m} \quad \text{..... (2)}$$

$$\upsilon_{12} = V_{CNT}^{*}\upsilon_{12}^{CNT} + V_m\upsilon^m$$

$$\upsilon_{21} = \upsilon_{12}E_{22}/E_{11}$$

where E_{11}^{CNT} , E_{22}^{CNT} and G_{12}^{CNT} are the elastic and shear moduli of the CNT. E^mandG^m are the corresponding properties of the isotropic matrix. Since the load transfer between the CNT and matrix is less than perfect, the CNT efficiency parameters η_1 ,η_2 *and* η_3 are introduced to account for load transfer between the CNT and polymeric phases. V_{CNT} *and* $V_m$are the volume fractions of the CNT and matrix, and their sum must be equal to 1, that is $V_{CNT} + V_m = 1$.

A.Displacement model

In formulating the higher-order shear deformation theory, a plate of $0 \le x \le a\,; 0 \le y \le b$ and $-\frac{h}{2} \le z \le \frac{h}{2}$ is considered as shown in the Fig.2.

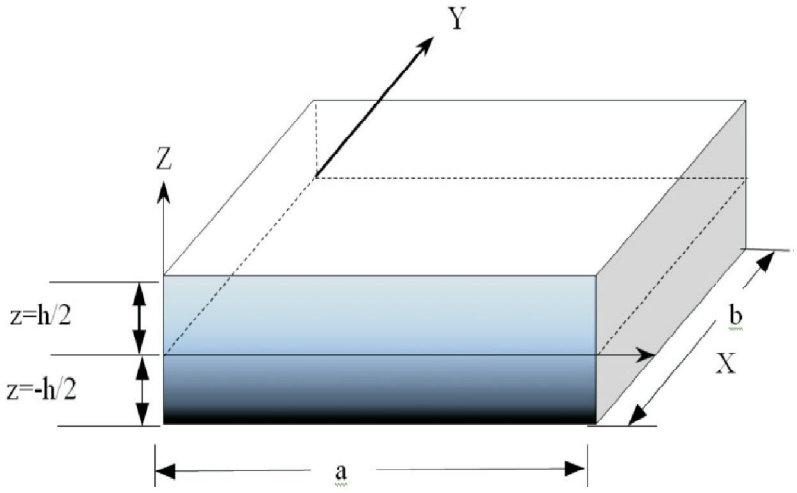

Fig.2Functionally graded plate with coordinates.

In order to approximate 3D-elasticity plate problem to a 2D one, the displacement components u (x, y, z), v (x, y, z) and w (x, y, z) at any point in the plate are expanded in terms of the thickness coordinate. The elasticity solution indicates that the transverse shear stress varies parabolically through the plate thickness. This requires the use of a displacement field, in which the in-plane displacements are expanded as cubic functions of the thickness coordinate. The displacement field which assumes w (x, y, z) constant through the plate thickness thus setting $\varepsilon_z = 0$ is expressed as:

$$\left.\begin{aligned} u(x,y,z) &= u_o(x,y) + z\theta_x(x,y) + z^2u_o^*(x,y) + z^3\theta_x^*(x,y) \\ v(x,y,z) &= v_o(x,y) + z\theta_y(x,y) + z^2v_o^*(x,y) + z^3\theta_y^*(x,y) \\ w(x,y,z) &= w_o(x,y) \end{aligned}\right\} \quad \text{..... (3)}$$

where, the parameters u_0, v_0, w_0 denote the displacements of a point (x, y) on the mid-plane. The functions θ_x,θ_y are rotations of the normal to the mid-plane about y and x axes, respectively. The parameters u_0^*, v_o^*, θ_x^*, $\theta_y^*$are the corresponding higher-order deformation terms.

In present work, analytical formulation and solution were obtained without enforcing zero transverse shear stress conditions on the top and bottom surfaces of the plate. In formulating the theory, the following assumptions are considered:

1) The layers are perfectly bonded together.
2) The material of each layer is linearly elastic and Orthotropic.
3) Each layer is of uniform thickness.

©IJRASET (UGC Approved Journal): All Rights are Reserved

4) The strains and displacements are small.

B. Strain- displacement Relations

The higher-order theories introduce additional unknowns that are often difficult to interpret in physical terms. The third order theory with transverse inextensibility based on the displacement field is shown in Eq.(3).

By substitution of the displacement relations in Eq.(3) in to strain displacement equations of the classical theory of elasticity the following relations are obtained:

$$\varepsilon_x = \varepsilon_{xo} + zk_x + z^2\varepsilon^*_{xo} + z^3k^*_x$$
$$\varepsilon_y = \varepsilon_{yo} + zk_y + z^2\varepsilon^*_{yo} + z^3k^*_y$$
$$\varepsilon_z = 0 \qquad \text{……...(3.a)}$$
$$\gamma_{xy} = \varepsilon_{xyo} + zk_{xy} + z^2\varepsilon^*_{xyo} + z^3k^*_{xy}$$
$$\gamma_{yz} = \phi_y + z\varepsilon_{yzo} + z^2\phi^*_y$$
$$\gamma_{xz} = \phi_x + z\varepsilon_{xzo} + z^2\phi^*_x$$

where,

$$\varepsilon_{xo} = \frac{\partial uo}{\partial x},\ \varepsilon_{yo} = \frac{\partial vo}{\partial y},\ \varepsilon_{xyo} = \frac{\partial uo}{\partial y} + \frac{\partial v_o}{\partial x}$$
$$k_x = \frac{\partial \theta_x}{\partial x},\ k_y = \frac{\partial \theta_y}{\partial y},\ k_{xy} = \frac{\partial \theta_x}{\partial y} + \frac{\partial \theta_y}{\partial x}$$
$$k^*_x = \frac{\partial \theta^*_x}{\partial x},\ k^*_y = \frac{\partial \theta^*_y}{\partial y},\ k^*_{xy} = \frac{\partial \theta^*_x}{\partial y} + \frac{\partial \theta^*_y}{\partial x}$$

$$\varepsilon^*_{xo} = \frac{\partial u^*_o}{\partial x},\ \varepsilon^*_{yo} = \frac{\partial v^*_o}{\partial y}, \varepsilon^*_{xyo} = \frac{\partial u^*_o}{\partial y} + \frac{\partial v^*_o}{\partial x},$$
$$\phi_y = \theta_y + \frac{\partial w_o}{\partial y},\ \phi_x = \theta_x + \frac{\partial w_o}{\partial x},$$
$$\varepsilon_{yzo} = 2v^*_o, \varepsilon_{xzo} = 2u^*_o,\ \phi^*_y = 3\theta^*_y,\ \phi^*_x = 3\theta^*_x$$

C. Constitutive Relations

Since $\varepsilon_z = 0$, the transverse normal stress σ_z, although not zero identically, does not appear in the virtual work statement and hence in the equations of motion. Consequently, it amounts to neglecting the transverse normal stress. Thus we have, in theory, a case of plane stress. For an FG-CNT reinforced composite plate, the plane stress reduced elastic constants and the transformed plane stress reduced elastic constants will be same i.e., $C_{ij} = Q_{ij}$. The linear constitutive relations for the coordinates (x-y-z) are:

$$\begin{Bmatrix}\sigma_x\\ \sigma_y\\ \tau_{xy}\end{Bmatrix}^L = \begin{bmatrix}Q_{11} & Q_{12} & 0\\ Q_{12} & Q_{22} & 0\\ 0 & 0 & Q_{33}\end{bmatrix}^L \begin{Bmatrix}\varepsilon_x\\ \varepsilon_y\\ \gamma_{xy}\end{Bmatrix}^L \qquad \text{.....(3.b)}$$

$$\begin{Bmatrix}\tau_{yz}\\ \tau_{xz}\end{Bmatrix}^L = \begin{bmatrix}Q_{44} & 0\\ 0 & Q_{55}\end{bmatrix}^L \begin{Bmatrix}\gamma_{yz}\\ \gamma_{xz}\end{Bmatrix}^L$$

where $\sigma_x, \sigma_y, \tau_{xy}, \tau_{yz}, \tau_{xz}$ are the stresses and $\varepsilon_x, \varepsilon_y, \gamma_{xy}, \gamma_{yz}, \gamma_{xz}$ are the linear strains with respect to the local reference axes. Q_{ij} are the transformed plane stress reduced elastic constants in the plate axes of the composite plate.

$$Q_{11} = \frac{E_{11}}{(1-\upsilon_{12}\upsilon_{21})},\qquad Q_{22} = \frac{E_{22}}{(1-\upsilon_{12}\upsilon_{21})},\qquad Q_{12} = \frac{\upsilon_{21}E_{11}}{(1-\upsilon_{12}\upsilon_{21})},$$

$$Q_{33} = G_{12}, Q_{44} = G_{23}, Q_{55} = G_{13}$$

©IJRASET (UGC Approved Journal): All Rights are Reserved

where,

E_{ii} = Young's modulus of elasticity in the i direction.

υ_{ij} = Poisson's ratios that give strain in the j direction due to stress in the i direction.

G_{ij} = shear moduli.

D. Equations of motion

The work done by actual forces in moving through virtual displacements, that are consistent with the geometric constraints of a body is set to zero to obtain the equations of motion and this is known as energy principle. It is useful in deriving governing equations, boundary conditions and obtaining approximate solutions by virtual methods.

Governing equations of higher-order theory for Eq.(3) will be derived using the dynamic version of the principle of virtual displacements, i.e.

$$\int_0^T (\delta U + \delta V - \delta K)\, dt = 0 \qquad \text{.....(3.c)}$$

where,

δU = Virtual strain energy

δV = Virtual work done by applied forces

δK = Virtual kinetic energy

$\delta U+\delta V$=total potential energy

The virtual strain energy, work done and kinetic energy are given by

$$\delta U = \int_A \left\{ \int_{-h/2}^{h/2} \left[\sigma_x \delta\varepsilon_x + \sigma_y \delta\varepsilon_y + \tau_{xy}\delta\gamma_{xy} + \tau_{xz}\delta\gamma_{xz} + \tau_{yz}\delta\gamma_{yz}\right] dz \right\} dx\, dy$$

$$\delta \mathbf{V} = -\int \boldsymbol{q}\,\delta \boldsymbol{w0}\, \boldsymbol{dx}\, \boldsymbol{dy} \qquad \text{…….(3.d)}$$

$$\delta K = \int_A \{ \int_{-h/2}^{h/2} \rho_0 \left[\left(\dot{u}_0 + Z\dot{\theta}_x + Z^2 \dot{u}_0^{\,*} + Z^3 \dot{\theta}_x^{\,*}\right)\left(\delta\dot{u}_0 + Z\delta\dot{\theta}_x + Z^2 \delta\dot{u}_0^{\,*} + Z^3 \delta\dot{\theta}_x^{\,*}\right) + \left(\dot{v}_0 + Z\dot{\theta}_y + Z^2 \dot{v}_0^{\,*} + Z^3 \dot{\theta}_y^{\,*}\right)\left(\delta\dot{v}_0 + Z\delta\dot{\theta}_y + Z^2\delta \dot{v}_0^{\,*} + Z^3\delta \dot{\theta}_y^{\,*}\right) + \dot{w}_0 \delta\dot{w}_0 \right] dz \}\, dx\, dy$$

where,

q = distributed load over the surface of the plate.

ρ_0 = Density of plate material

$\dot{u}_0 = \partial u_0 / \partial t$, $\dot{v}_0 = \partial v_0 / \partial t$ etc. indicates the time derivatives

On substituting for δU, δV and δK from Eq. (3.d) in to the virtual work statement in Eq. (3.c) and integrating through the thickness of the plate and rewriting in a matrix form which defines the stress/strain relations of the plate are given by:

$$\begin{Bmatrix} N \\ N^* \\ -- \\ M \\ M^* \\ -- \\ Q \\ Q^* \end{Bmatrix} = \left[\begin{array}{c|c|c} A & B & 0 \\ \hline B^t & D_b & 0 \\ \hline 0 & 0 & D_s \end{array}\right] \begin{Bmatrix} \varepsilon_0 \\ \varepsilon_0^* \\ -- \\ K \\ K^* \\ -- \\ \phi \\ \phi^* \end{Bmatrix} \qquad \text{……. (3.e)}$$

©IJRASET (UGC Approved Journal): All Rights are Reserved

Where, the in-plane force and moment resultants are defined as:

$$\begin{Bmatrix} N_x & | & N_x^* \\ N_y & | & N_y^* \\ N_{xy} & | & N_{xy}^* \end{Bmatrix} = \sum_{L=1}^{n} \int_{h_{L-1}}^{h_L} \begin{Bmatrix} \sigma_x \\ \sigma_y \\ \tau_{xy} \end{Bmatrix} \left[1 \mid z^2\right] dz$$

$$\begin{Bmatrix} M_x & | & M_x^* \\ M_y & | & M_y^* \\ M_{xy} & | & M_{xy}^* \end{Bmatrix} = \sum_{L=1}^{n} \int_{h_{L-1}}^{h_L} \begin{Bmatrix} \sigma_x \\ \sigma_y \\ \tau_{xy} \end{Bmatrix} \left[Z \mid Z^3\right] dz$$

Transverse force resultants and the inertias are given by:

$$\begin{Bmatrix} Q_x & | & S_x & | & Q_x^* \\ Q_y & | & S_y & | & Q_y^* \end{Bmatrix} = \sum_{L=1}^{n} \int_{h_{L-1}}^{h_L} \begin{Bmatrix} \tau_{xz} \\ \tau_{yz} \end{Bmatrix} \left[1 \mid Z \mid Z^2\right] dz \, I_1, I_2, I_3, I_4, I_5, I_6, I_7 = \int_{-h/2}^{h/2} \rho_0 (1, z, z^2, z^3, z^4, z^5, z^6) \, dz$$

Also, $\varepsilon_0 = [\varepsilon_{x0} \;\; \varepsilon_{y0} \;\; \varepsilon_{xy0}]^t \; ; \varepsilon_0^* = [\varepsilon_{x0}^* \;\; \varepsilon_{y0}^* \;\; \varepsilon_{xy0}^*]^t$

$$k = [k_x \;\; k_y \;\; k_{xy}]^t \; ; k^* = [k_x^* \;\; k_y^* \;\; k_{xy}^*]^t$$

$$\phi = [\phi_x \;\; \phi_y]^t \; ; \phi^* = [\varepsilon_{xz0} \;\; \varepsilon_{yz0} \;\; \phi_x^* \;\; \phi_y^*]^t$$

Integrating the above equation by parts and collecting coefficients of each of virtual displacements $\delta u_0 \delta v_0$, δw_0, $\delta\theta_x$, $\delta\theta_y$, δu_0^*, δv_0^*, $\delta\theta_x^*$, $\delta\theta_y^*$ together and virtual displacements are zero, the following equations of motion are obtained as:

$$\delta u_0 : \frac{\partial N_x}{\partial x} + \frac{\partial N_{xy}}{\partial y} = I_1 \ddot{u}_0 + I_2(\ddot{\theta}_x) + I_3 \ddot{u}_0^* + I_4 \ddot{\theta}_x^*$$

$$\delta v_0 : \frac{\partial N_y}{\partial y} + \frac{\partial N_{xy}}{\partial x} = I_1 \ddot{v}_0 + I_2(\ddot{\theta}_y) + I_3 \ddot{v}_0^* + I_4 \ddot{\theta}_y^*$$

$$\delta w_0 : \frac{\partial Q_x}{\partial x} + \frac{\partial Q_y}{\partial y} + q = I_1 \ddot{w}_0$$

$$\delta\theta_x : \frac{\partial M_x}{\partial x} + \frac{\partial M_{xy}}{\partial y} - Q_x = I_2 \ddot{u}_0 + I_3(\ddot{\theta}_x) + I_4 \ddot{u}_0^* + I_5 \ddot{\theta}_x^* \qquad \text{..... (3.f)}$$

$$\delta\theta_y : \frac{\partial M_y}{\partial y} + \frac{\partial M_{xy}}{\partial x} - Q_y = I_2 \ddot{v}_0 + I_3(\ddot{\theta}_y) + I_4 \ddot{v}_0^* + I_5 \ddot{\theta}_y^*$$

$$\delta u_0^* : \frac{\partial N_x^*}{\partial x} + \frac{\partial N_{xy}^*}{\partial y} - 2S_x = I_3 \ddot{u}_0 + I_4(\ddot{\theta}_x) + I_5 \ddot{u}_0^* + I_6 \ddot{\theta}_x^*$$

$$\delta v_0^* : \frac{\partial N_y^*}{\partial y} + \frac{\partial N_{xy}^*}{\partial x} - 2S_y = I_3 \ddot{v}_0 + I_4(\ddot{\theta}_y) + I_5 \ddot{v}_0^* + I_6 \ddot{\theta}_y^*$$

$$\delta\theta_x^* : \frac{\partial M_x^*}{\partial x} + \frac{\partial M_{xy}^*}{\partial y} - 3Q_x^* = I_4 \ddot{u}_0 + I_5(\ddot{\theta}_x) + I_6 \ddot{u}_0^* + I_7 \ddot{\theta}_x^*$$

$$\delta\theta_y^* : \frac{\partial M_y^*}{\partial y} + \frac{\partial M_{xy}^*}{\partial x} - 3Q_y^* = I_4 \ddot{v}_0 + I_5(\ddot{\theta}_y) + I_6 \ddot{v}_0^* + I_7 \ddot{\theta}_y^*$$

IV. ANALYTICAL SOLUTIONS

Composite rectangular plates are generally classified by referring to the type of support used. The analytical solutions of the Eq. (7) (12) for simply supported FG-CNT plates are dealt here. Assuming that the plate is simply supported in such a manner that normal displacement is admissible, but the tangential displacement is not, solution functions that completely satisfy the boundary conditions in the equations below are assumed as follows:

©IJRASET (UGC Approved Journal): All Rights are Reserved

$$u_0(x,y)=\sum_{m=1}^{\infty}\sum_{n=1}^{\infty}U_{mn}\cos\alpha x\sin\beta y$$

$$v_0(x,y)=\sum_{m=1}^{\infty}\sum_{n=1}^{\infty}V_{mn}\sin\alpha x\cos\beta y$$

$$w_0(x,y)=\sum_{m=1}^{\infty}\sum_{n=1}^{\infty}W_{mn}\sin\alpha x\sin\beta y$$

$$\theta_x(x,y)=\sum_{m=1}^{\infty}\sum_{n=1}^{\infty}X_{mn}\cos\alpha x\sin\beta y$$

$$\theta_y(x,y)=\sum_{m=1}^{\infty}\sum_{n=1}^{\infty}Y_{mn}\sin\alpha x\cos\beta y \qquad \text{……. (4)}$$

$$u_0^*(x,y)=\sum_{m=1}^{\infty}\sum_{n=1}^{\infty}U_{mn}^*\cos\alpha x\sin\beta y$$

$$v_o^*(x,y)=\sum_{m=1}^{\infty}\sum_{n=1}^{\infty}V_{mn}^*\sin\alpha x\cos\beta y$$

$$\theta_x^*(x,y)=\sum_{m=1}^{\infty}\sum_{n=1}^{\infty}X_{mn}^*\cos\alpha x\sin\beta y$$

$$\theta_y^*(x,y)=\sum_{m=1}^{\infty}\sum_{n=1}^{\infty}Y_{mn}^*\sin\alpha x\cos\beta y$$

for $\mathbf{0}\le \boldsymbol{x}\le \boldsymbol{a}\,;\mathbf{0}\le \boldsymbol{y}\le \boldsymbol{b}$

The mechanical load is expanded in double Fourier sine series as:

$$q(x,y)=\sum_{m=1}^{\infty}\sum_{n=1}^{\infty}Q_{mn}\sin\alpha x\sin\beta y \qquad \text{……. (5)}$$

Where,

$\alpha=\frac{m\pi}{a}$ and $\beta=\frac{n\pi}{b}$ and *m* and *n* are modes numbers, and ω is the natural frequency of the system.

We may obtain the natural frequencies and vibration modes for the plate by solving the Eigen value problem $([S]-\omega^2[M])\,X=0$, where X are the modes of vibration associated with the natural frequencies defined as ω.

V. RESULTS AND DISCUSSIONS

A. Comparative Study

In this section, in order to validate the accuracy of the present higher-order shear deformation theory in predicting the frequencies of a simply supported functionally graded CNT reinforced composite plates, examples are presented and discussed.

Poly{(m-phenylenevinylene)-co-[(2,5-dioctoxy-p-phenylene) vinylene]} referred as PmPV is selected as the matrix. The material properties of which are as follows:

$E^m = 2.1\ GPa$, $\rho^m = 1.15\frac{g}{cm^3}$, $\vartheta^m = 0.34$

SWCNT (single-walled carbon nanotubes) are taken as the reinforcements and its properties are:

$E_{11}^{CNT} = 5.6466\ TPa$, $E_{22}^{CNT} = 7.0800 TPa$,

$G_{12}^{CNT} = 1.9445\ TPa$, $\upsilon_{12}^{CNT} = 0.175$

and $\rho^{CNT} = 1400\ kg/m^3$ [15].

©IJRASET (UGC Approved Journal): All Rights are Reserved

The CNT efficiency parameters for different volume fractions are presented in TABLE I. It is assumed that the effective shear moduli $G_{13} = G_{23} = G_{12}$ *and* $\eta_3 = \eta_2$.

TABLE I
EFFICIENCY PARAMETERS OF SWCNTS [17]

V^*_{CNT}	η_1	η_2	η_3
0.11	0.149	0.934	0.934
0.14	0.150	0.941	0.941
0.17	0.149	1.381	1.381

Presently computed results for different values of volume fraction and side-to-thickness ratios (*a*/*h*) are compared with those of L.W.Zhang et al.[3] (here considered to be the exact solution) and presented in Table II.

For convenience, natural frequency ω has been non-dimensional zed as $\bar{\omega} = \omega h\sqrt{\rho_m/E_m}$.

From Table II, it can be observed that the values are in agreement with L.W.Zhang et al.[3] in which the Reddy's third order theory was used for the analysis purpose.

TABLE II
COMPARISON OF NON-DIMENSIONAL NATURAL FREQUENCY ($\bar{\omega} = \omega h\sqrt{\rho_m/E_m}$) SUBJECTED TO SINUSOIDAL LOADING

Volume Fraction =0.11	a/h = 5		a/h = 10	
	Present	L.W.Zhang et al.[3]	Present	L.W.Zhang et al.[3]
UD	0.886	0.890	1.372	1.373
FG-X	0.906	0.923	1.487	1.489

B. Parametric Study

The variation of Fundamental frequency with the change in side-to-thickness ratio and for different CNT distributions at various volume fractions are presented in TABLE III. These results are plotted and compared with the standard values.

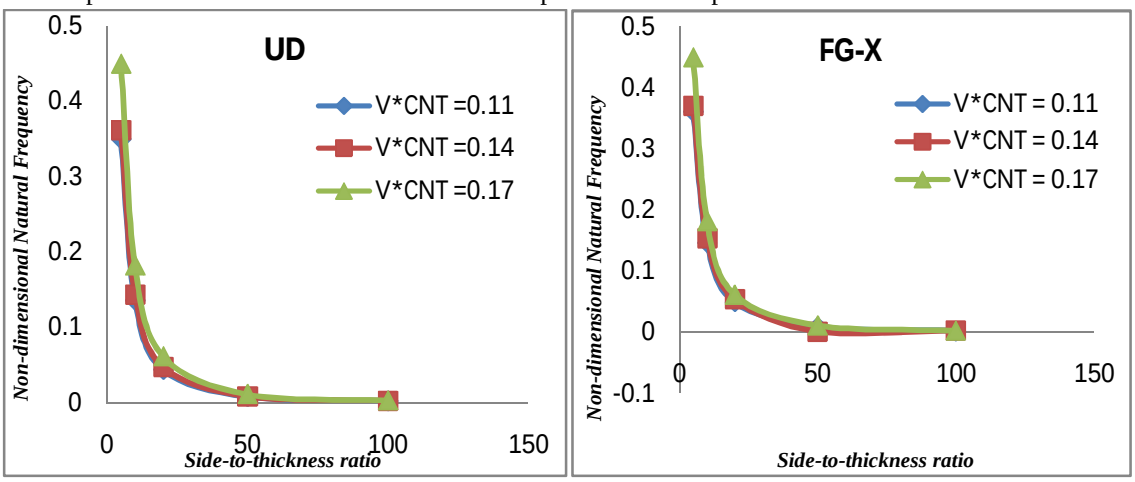

Fig.3 Effect of aspect ratios on the non-dimensional natural frequency ($\bar{\omega} = \omega h\sqrt{\rho_m/E_m}$) of a FG-CNT plate at different volume fractions

Fig.3 shows the variation of the non-dimensional natural frequency with respect to side-to-thickness ratios (*a*/*h*) for various distributions of CNT, according to present higher-order shear deformation theory. From this, it is clear that the effect of decreasing

©IJRASET (UGC Approved Journal): All Rights are Reserved

frequencies is felt with the increase in a/h ratio for simply supported boundary conditions. The effect of shear deformation decreases with the increasing values of *a*/*h* and decreasing values of volume fractions.

TABLE III

NON-DIMENSIONAL NATURAL FREQUENCY ($\bar{\omega} = \omega h\sqrt{\rho_m/E_m}$) OF FG-CNT COMPOSITE PLATE FOR VARIOUS DISTRIBUTIONS AT DIFFERENT ASPECT RATIOS SUBJECTED TO SINUSOIDAL LOADING

Side-to-thickness ratio	Type of Distribution	V = 0.11	V = 0.14	V = 0.17
5	UD	0.349878	0.361866	0.436903
	FG-X	0.361422	0.372078	0.449779
10	UD	0.135422	0.143636	0.168278
	FG-X	0.146744	0.153848	0.181821
20	UD	0.043290	0.047286	0.053502
	FG-X	0.049728	0.053946	0.061495
50	UD	0.007548	0.008436	0.009324
	FG-X	0.009341	0.001021	0.011100
100	UD	0.001998	0.002220	0.002442
	FG-X	0.002442	0.002664	0.002886

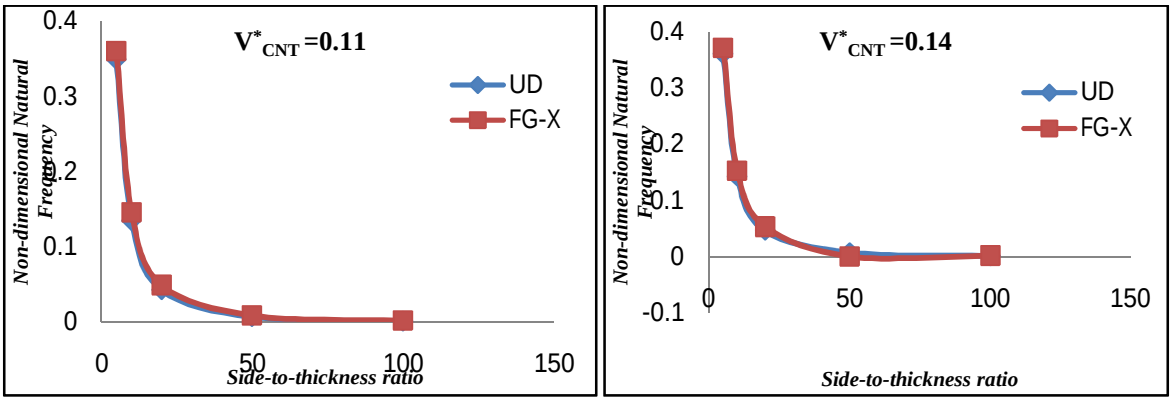

Fig.4Comparison of non-dimensional natural frequency ($\bar{\omega} = \omega h\sqrt{\rho_m/E_m}$) of FG-CNT plate for different distributions at $V^*_{CNT} = 0.11$ and $V^*_{CNT} = 0.14$

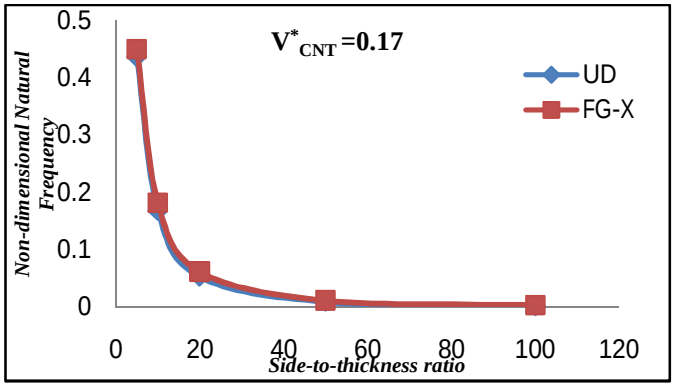

Fig.5Comparison of non-dimensional natural frequency ($\bar{\omega} = \omega h\sqrt{\rho_m/E_m}$) of FG-CNT plate for different distributions at $V^*_{CNT} = 0.17$

©IJRASET (UGC Approved Journal): All Rights are Reserved

Fig.4 and Fig.5 shows the comparison of $\bar{\omega}$of FG-CNT plate for different distributions at various volume fractions. It is clear from these plots that X-distribution is more effective than the uniform distribution of CNT as the variation of $\bar{\omega}$ is consistent for FG-X.

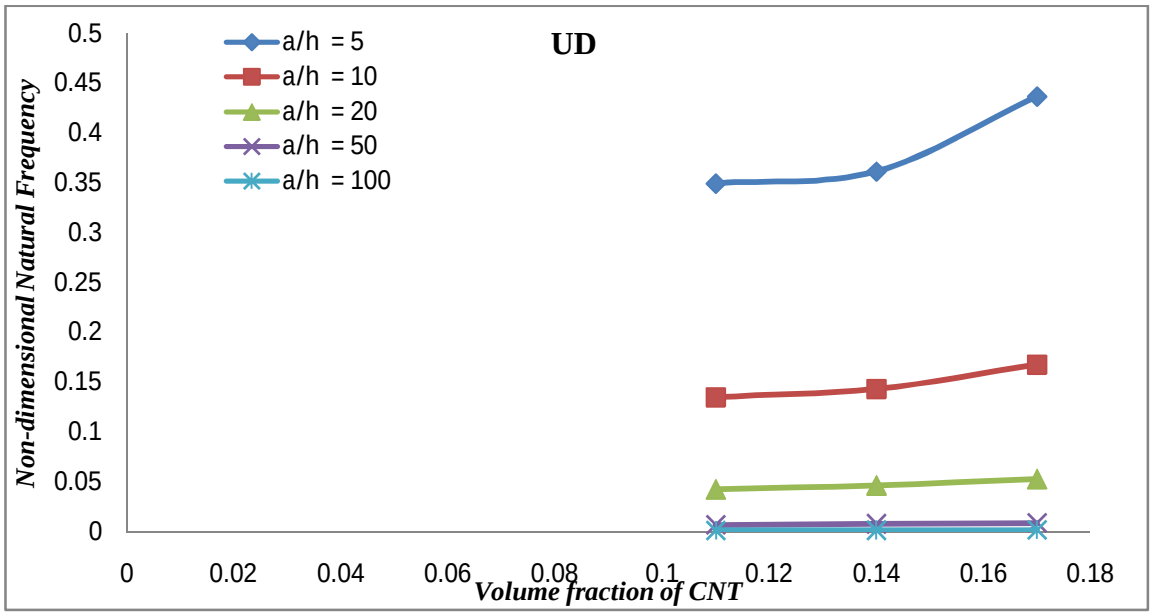

Fig.6Effect of volume fractions on the non-dimensional natural frequency ($\bar{\omega} = \omega h\sqrt{\rho_m/E_m}$) of a uniformly distributed FG-CNT plate for different values of aspect ratios

In Fig.6 and Fig.7, it is observed that with the increase in a/h ratio, the value of fundamental frequency decreases and for a particular a/h value, with the increase in volume fraction of CNT, the value of fundamental frequency increases.

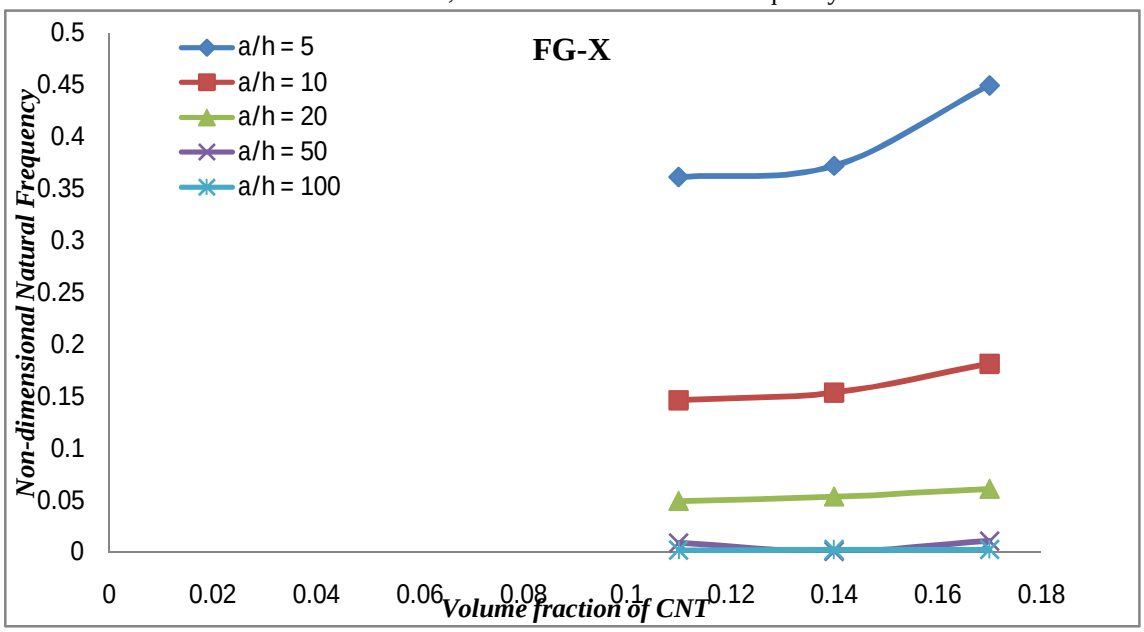

Fig.7 Effect of volume fractions on the non-dimensional natural frequency ($\bar{\omega} = \omega h\sqrt{\rho_m/E_m}$) of a FG-X CNT reinforced composite plate for different values of aspect ratios

It is also clear from the graph that the effect of side-to-thickness ratio increases the change in fundamental frequency. That is, the rate of change in fundamental frequency increases when we go to the higher values of a/h values.

©IJRASET (UGC Approved Journal): All Rights are Reserved

VI. CONCLUSIONS

Formulations and solutions for free vibration behaviour of FG-CNT reinforced composite plate is developed using the higher-order shear deformation theory considering the which account for transverse extensibility and without enforcing zero shear on the top and bottom of the FG-CNT plates. Hamilton's principle is used in deriving the equations of motion. Closed form solutions are obtained for simply supported boundary conditions using Naviers method and solving the eigen value problem. The accuracy and efficiency of the present theory have been demonstrated in the results and discussions of the FG-CNT plates. The results are compared with the other higher order shear deformation theory and are in good agreement with those L.W. Zhang et al.[3] which are validated and confirmed to be accurate. Hence, the present results which are obtained using this theory can be used as reference for further studies. From the above, it can be concluded that the proposed theory is simple and accurate in analyzing the free vibration behavior of FG-CNT composite plates.

REFERENCES

[1] HassenAitAtmane, AbdelouahedTounsi, Sid Ahmed Meftah and Hichem Abdesselem Belhadj, Free Vibration Behavior of Exponential Functionally Graded Beams with Varying Cross-section, Journal of Vibration and Control 2011 17: 311.
[2] Udupa G, Rao SS, Gangadharan KV**,** Fabrication of Functionally Graded Carbon Nanotube-Reinforced Aluminium Matrix Laminate by Mechanical Powder Metallurgy Technique - Part I, Journal of Material Sciences & Engineering,4:3.
[3] Zhang, L.W., Song, Z.G., Liew, K.M.,(2015) State-space Levy method for vibration analysis of FG-CNT composite plates subjected to in-plane loads based on higher-order shear deformation theory, Composite Structures
[4] .A. Fazelzadeh, S. Pouresmaeeli, E. Ghavanloo, Aeroelastic characteristics of functionally graded carbon nanotube-reinforced composite plates under a supersonic flow, Comput. Methods Appl. Mech. Engrg. 285 (2015) 714–729.
[5] Pindera, M.-J., Aboudi, J, Glaeser, A M., and Arnold, S. M, Use of Composites in Multi-Phased and Functionally Graded Materials, Composites, Part B 28, pp. 1-175,1997.
[6] Suresh, S., and Mortensen, A, Fundamentals of Functionally Graded Materials, 10M Communications, London, 1998.
[7] Liew KM, Lei ZX and Zhang L W 2015 Mechanical analysis of functionally graded carbon nanotube reinforced composites: A review. Compos. Struct. 120**,** 90-97
[8] Zhu P, Lei ZX, Liew KM. Static and free vibration analyses of carbon nanotube-reinforced composite plates using finite element method with first order shear deformation plate theory. Compos Struct. Volume 94, Issue 4, March 2012, Pages 1450–1460.
[9] Zhang, L.W., Lei, Z.X., Liew, K.M., Free vibration analysis of functionally graded carbonnanotube-reinforced composite triangular plates using the FSDT and element-free IMLS-Ritz method, CompositeStructures (2014).
[10] Liao-Liang Ke, Jie Yang, SritawatKitipornchai, Nonlinear free vibration of functionally graded carbon nanotube-reinforced composite beams,, Composite Structures 92 (2010) 676–683.
[11] Yas M H, Pourasghar A, Kamarian S and Heshmati M 2013 Three-dimensional free vibration analysis of functionally graded nanocomposite cylindrical panels reinforced by carbon nanotube, Mater. Design49 583-590.
[12] Heshmati M, Yas M H and Daneshmand F 2015 A comprehensive study on the vibrational behavior of CNT-reinforced composite beams Composite Structures 125 434-448.
[13] .Kant, K.Swaminathan, Analytical solutions for free vibration of laminated composite and sandwich plates based on a higher-order refined theory, Composite Structures 53 (2001) 73-85.Arvind Agarwal, SrinivasaRaoBakshi,DebrupaLahiri "Carbon Nanotubes Reinforced Metal Matrix Composites", CRC press.
[14] Zhu J, Yang J and Kitipornchai S 2013 Dispersion spectrum in a functionally graded carbon nanotube-reinforced plate based on first-order shear deformation plate theory Compos. Part B 53 274-283.
[15] Shen H S and Zhang C L 2010 Thermal buckling and postbuckling behavior of functionally graded carbon nanotube-reinforced composite plates Mater. Des.31 3403-3411.
[16] M. Mohammadimehr, M. Salemi, B. RoustaNavi (15 March 2016), Bending, buckling, and free vibration analysis of MSGTmicrocomposite Reddy plate reinforced by FG-SWCNTs with temperature dependent material properties under hydro-thermo-mechanical loadings using DQM, Composite structures, Volume 138, Pages 361–380.

©IJRASET (UGC Approved Journal): All Rights are Reserved

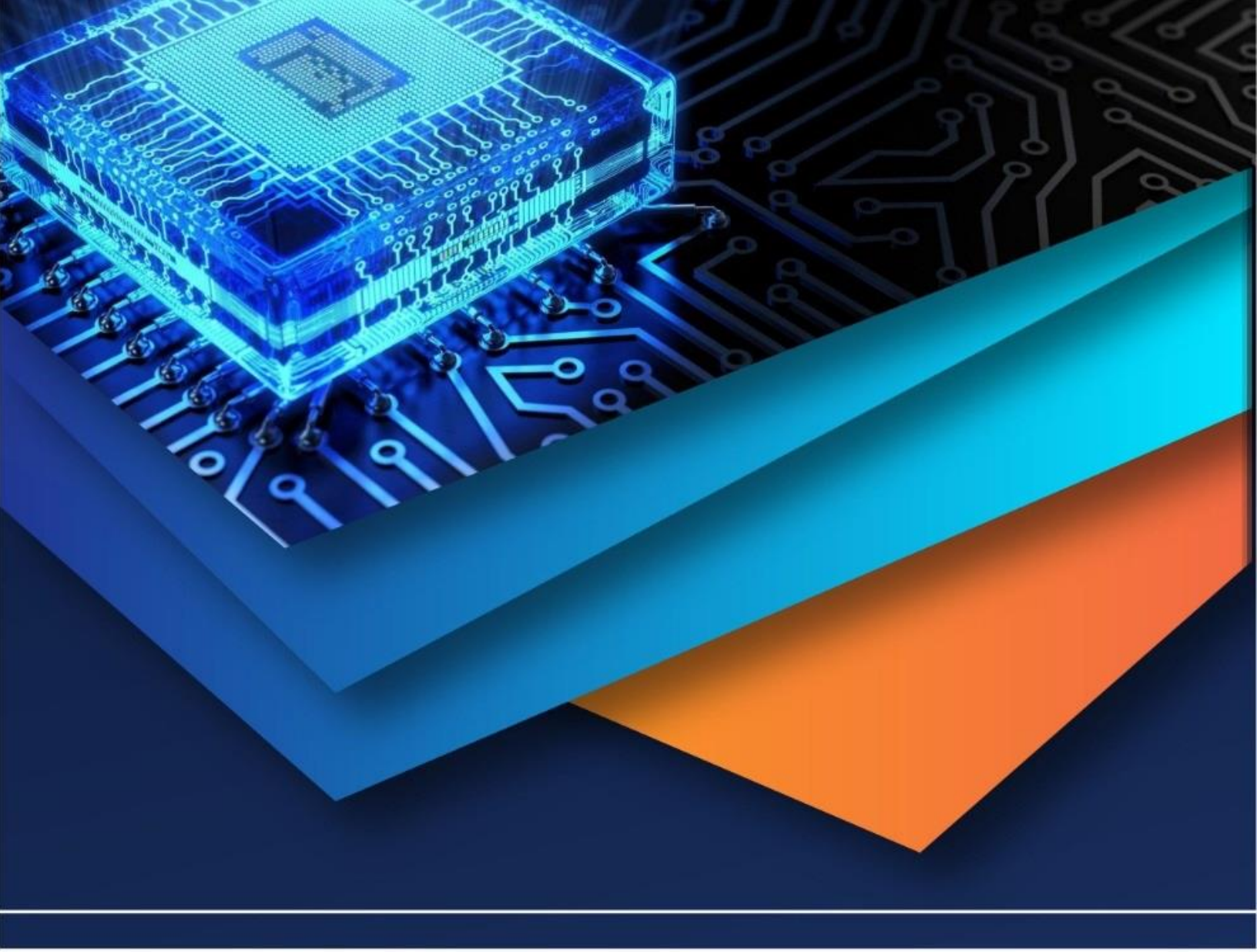

10.22214/IJRASET

45.98

IMPACT FACTOR: 7.129

IMPACT FACTOR: 7.429

INTERNATIONAL JOURNAL FOR RESEARCH

IN APPLIED SCIENCE & ENGINEERING TECHNOLOGY

Call : 08813907089 (24*7 Support on Whatsapp)